nels, in a manner analogous to those in CNG channels, will be responsible for their proton sensitivity.

REFERENCES AND NOTES

1. R. W. Tsien, P. Hess, E. W. McCleskey, R. L. Rosenberg, *Annu. Rev. Biophys. Biophys. Chem.* **16**, 265 (1987); G. Colamartino, A. Menini, V. Torre, *J. Physiol.* **440**, 189 (1991); F. Zufall and S. Firestein, *J. Neurophysiol.* **69**, 1758 (1993).
2. K.-W. Yau and D. A. Baylor, *Annu. Rev. Neurosci.* **12**, 289 (1989).
3. U. B. Kaupp and K.-W. Koch, *Annu. Rev. Physiol.* **54**, 153 (1991); R. H. Kramer and S. A. Siegelbaum, *Neuron* **9**, 897 (1992); T.-Y. Chen and K.-W. Yau, *Nature* **368**, 545 (1994).
4. L. Heginbotham, T. Abramson, R. MacKinnon, *Science* **258**, 1152 (1992).
5. M.-S. Kim, T. Morii, L.-X. Sun, K. Imoto, Y. Mori, *FEBS Lett.* **318**, 145 (1993); G. Mikala, A. Bahinski, A. Yatani, S. Tang, A. Schwartz, *ibid.* **335**, 265 (1993); J. Yang, P. T. Ellinor, W. A. Sather, J.-F. Zhang, R. W. Tsien, *Nature* **366**, 158 (1993).
6. M. J. Root and R. MacKinnon, *Neuron* **11**, 459 (1993); E. Eismann, F. Muller, S. H. Heinemann, U. B. Kaupp, *Proc. Natl. Acad. Sci. U.S.A.* **91**, 1109 (1994).
7. E. H. Goulding *et al.*, *Neuron* **8**, 45 (1992).
8. W. P. Jencks, *Catalysis in Chemistry and Enzymology* (Dover, New York, 1987).
9. S. D. Tyerman, B. R. Terry, G. P. Findlay, *Biophys. J.* **61**, 736 (1992).
10. In this paper, we cite the directly measured pH; for pure ^2H_2O solutions, this value is an overestimate of the actual free $^2H^+$ concentration [L. Pentz and E. R. Thornton, *J. Am. Chem. Soc.* **86**, 6931 (1967)]. The actual value of $-\log[^2H^+]$ can be estimated by adding 0.4 units to the cited pH.
11. The transfer could be direct or be mediated by one or more H_2O molecules between the H^+ donor and acceptor [R. P. Bell, *The Proton in Chemistry* (Cornell Univ. Press, Ithaca, NY, ed. 2, 1973); E. Caldin and V. Gold, Eds., *Proton Transfer Reactions* (Wiley, New York, 1975)].
12. The measured pK_{aB} of Hepes in ^2H_2O solutions is 7.74. It was determined by titration of a 30 mM Hepes solution with NaOH.
13. Microscopic reversibility would require that $\alpha\beta'K_{aB} = \alpha'\beta$. The rate constant magnitudes indicate that the system is out of equilibrium because of a "thermodynamic force" of about $1\ k_BT$, where k_B is the Boltzmann constant and T is absolute temperature. The observation is explicable because the membrane is held at −80 mV, and some protons exit to the inside. We discuss the results as if the system is at equilibrium, because our conclusions about the channel do not depend on the equilibrium condition. There is a twofold discrepancy between the K_a determined from the amplitude histogram analysis and that determined from the kinetic rate constants. We attribute this discrepancy to different systematic errors in the two measurements.
14. A. Fersht, *Enzyme Structure and Mechanism* (Freeman, New York, ed. 2, 1985).
15. H. H. Kohler and K. Heckmann, *J. Theor. Biol.* **79**, 381 (1979); M. F. Schumaker and R. MacKinnon, *Biophys. J.* **58**, 975 (1990); C. M. Armstrong and J. Neyton, *Ann. N.Y. Acad. Sci.* **635**, 18 (1991).
16. L. Sawyer and M. N. G. James, *Nature* **295**, 79 (1982).
17. D. L. D. Caspar and K. Namba, *Adv. Biophys.* **26**, 157 (1990).
18. O. Herzberg and M. N. G. James, *J. Mol. Biol.* **203**, 761 (1988); A. R. Sielecki *et al.*, *ibid.* **134**, 781 (1979); S. Mangani, P. Carloni, P. Orioli, *ibid.* **223**, 573 (1992).
19. C. A. Collyer, J. M. Guss, Y. Sugimura, F. Yoshizaki, H. C. Freeman, *ibid.* **211**, 617 (1990).
20. D. Pietrobon, B. Prod'hom, P. Hess, *J. Gen. Physiol.* **94**, 1 (1989); B. Prod'hom, D. Pietrobon, P. Hess, *ibid.*, p. 23.
21. The DNA construct for the olfactory CNG channel in the high-expression pGemHE vector was kindly provided by E. Goulding and S. Siegelbaum of Columbia University (*7*). RNA was synthesized from Sph 1–linearized DNA (New England Biolabs) with T7 polymerase (Promega). *Xenopus* oocytes (Xenopus One, Ann Arbor, MI) were prepared and injected with RNA as previously described [R. MacKinnon, P. H. Reinhart, M. M. White, *Neuron* **1**, 997 (1988)]. Inside-out patches were obtained with glass electrodes (Drummond, Broomall, PA) coated with either beeswax or Sylgard and firepolished to a resistance of 1 to 5 megohm. Single-channel currents were recorded with an Axopatch 200 (Axon Instruments) amplifier. The output of the amplifier was filtered at 1 or 2 kHz (3 dB corner frequency, 4-pole Bessel) and sampled (Indec Systems, Model IDA12120) at a frequency 7.15 times greater than the filter frequency.
22. For most electrophysiological experiments, both internal (bath) and external (pipette) solutions contained 130 mM NaCl, 3 mM Hepes, and 0.5 mM Na_2EDTA dissolved in either H_2O or ^2H_2O (99.9% atom D). To activate the channels, 1 mM Na · cyclic guanosine 3′,5′ monophosphate (Sigma) was added to the internal solution. The internal and external solutions were titrated to the indicated pH with NaOH or HCl. For ^2H_2O solutions, the fraction of contaminating hydrogens from Hepes, NaOH, and HCl did not exceed 0.05% of the total hydrogen and deuterium. The solution pH was measured with an Orion pH meter (Model 720) with a Corning electrode (no. 476540) that was routinely calibrated with pH 4, pH 7, and pH 10 H_2O buffers.
23. Our ability to measure the calculated protonation and deprotonation rates was tested by computer simulation of the open state of a single olfactory channel. Assuming scheme 6 with time constants comparable to measured values, a current template with Gaussian noise was generated, digitally filtered, and sampled, and then run through the same analysis programs. The simulation results showed that the time resolution of the recording system was sufficient to give the values of the rates reported here. Missed events and noise do cause minor deviations in the simulated rates; these deviations are qualitatively similar to deviations of the real data from the theoretical curves in Fig. 3, C through E.
24. Cassette mutants of the pore (Mlu I–Cla I) were generated by means of polymerase chain reaction (Ericomp; Perkin Elmer reagents) and were subcloned into the channel DNA. Mutations were confirmed by dideoxy sequencing between the restriction sites [F. Sanger, S. Nicklen, A. R. Coulson, *Proc. Natl. Acad. Sci. U.S.A.* **74**, 5463 (1977)].

25. We thank W. P. Jencks, J. Hogle, and P. Chen for helpful discussions and B. Bean, A. Gross, and L. Heginbotham for critical review of the manuscript. Supported by NIH research grant GM47400. M.J.R. was supported by NRSA Molecular Biophysics Training Grant 5 T32 GM083113.

14 April 1994; accepted 3 August 1994

RPS2 of *Arabidopsis thaliana*: A Leucine-Rich Repeat Class of Plant Disease Resistance Genes

Andrew F. Bent,* Barbara N. Kunkel,† Douglas Dahlbeck, Kit L. Brown,‡ Renate Schmidt, Jerome Giraudat, Jeffrey Leung, Brian J. Staskawicz§

Plant disease resistance genes function in highly specific pathogen recognition pathways. *RPS2* is a resistance gene of *Arabidopsis thaliana* that confers resistance against *Pseudomonas syringae* bacteria that express avirulence gene *avrRpt2*. *RPS2* was isolated by the use of a positional cloning strategy. The derived amino acid sequence of *RPS2* contains leucine-rich repeat, membrane-spanning, leucine zipper, and P loop domains. The function of the *RPS2* gene product in defense signal transduction is postulated to involve nucleotide triphosphate binding and protein-protein interactions and may also involve the reception of an elicitor produced by the avirulent pathogen.

Disease resistance genes control recognition of invading pathogens and subsequent activation of defense responses (*1*, *2*). Individual resistance genes are highly specific in function, being effective only against particular strains of a viral, bacterial, fungal, or nematode pathogen. For more than 80 years, crop breeding programs have used disease resistance genes because of their effectiveness in preventing disease and their ease of handling as single Mendelian loci. However, the molecular basis for resistance gene function is only starting to be elucidated.

Many plant pathogens produce specific elicitor compounds that are recognized by resistant plants, thereby triggering active defense responses that curtail pathogen growth (*1*–*3*). The pathogen genes that control production of these elicitors are known as avirulence genes, and the activity of a plant resistance gene is dependent on the presence of the specific, corresponding avirulence gene in the pathogen. Defense responses observed in infected tissue include production of antimicrobial compounds and cell wall–reinforcing proteins and a localized cell death response known as the hypersensitive response (*4*). The physiological mechanism by which these processes are activated is not clear, al-

A. F. Bent, B. N. Kunkel, D. Dahlbeck, K. L. Brown, B. J. Staskawicz, Department of Plant Biology, University of California, Berkeley, CA 94720, USA.
R. Schmidt, Cambridge Laboratory, John Innes Centre, Norwich NR4 7UJ, UK.
J. Giraudat and J. Leung, Institut des Sciences Végétales, Centre National de la Recherche Scientifique, 91198 Gif-sur-Yvette, France.

*Present address: Department of Agronomy, University of Illinois, Urbana, IL 61801, USA.
†Present address: Department of Biology, Washington University, St. Louis, MO 63130, USA.
‡Present address: Department of Microbiology, University of Washington, Seattle, WA 98195, USA.
§To whom correspondence should be addressed.

though a number of studies indicate that activated oxygen production, the gating of ion channels, and protein phosphorylation may be involved (*5*). Plant resistance genes have been postulated to encode receptors for the elicitors produced by avirulent pathogens (*1*, *3*), but to date no such receptors have been identified.

Two resistance genes have been characterized at the molecular level. *Hm1* from maize was isolated by the use of a transposon tagging strategy (*6*). This gene encodes a reductase that confers resistance against specific strains of the fungal pathogen *Cochliobolus carbonum* by degrading the fungal HC toxin, a resistance strategy that is mechanistically distinct from avirulence gene–dependent resistance. The *Pto* gene from tomato, which confers resistance against *Pseudomonas syringae* pv. *tomato* bacteria that express the *avrPto* avirulence gene, was recently isolated by positional cloning (*7*). The predicted *Pto* gene product resembles a serine-threonine protein kinase, which suggests (at least for this particular plant-pathogen interaction) that specific protein kinases play a critical role in the induction of host defenses. The cloning of additional resistance genes should greatly facilitate efforts both to understand the molecular basis of resistance and to use biotechnological strategies to improve field crop resistance (*1*, *2*).

The *RPS2* resistance gene of *Arabidopsis thaliana* confers resistance against *P. syringae* pv. *tomato* strains that express avirulence gene *avrRpt2* (*8*, *9*). Resistance against *P. syringae* pathogens expressing *avrRpt2* exists not only in *Arabidopsis*, but also in plant species such as soybean and bean (*10*, *11*). Prior genetic mapping had placed *RPS2* in the interval between restriction fragment length polymorphism (RFLP) markers λAt600 and λAt557 on *Arabidopsis* chromosome four, approximately 0.5 centimorgan (cM) from λAt600 (*8*, *9*). To proceed with map-based isolation of the *RPS2* gene, we used λAt600 as a hybridization probe to identify sets of yeast artificial chromosome (YAC) and cosmid clones that carry contiguous, overlapping inserts of *Arabidopsis* ecotype Col-0 genomic DNA (Fig. 1A) (*12*). Tightly linked RFLP markers generated from ends of insert DNA from the YAC and cosmid clones (Fig. 1A) were then used to localize *RPS2* to a 0.3-cM interval that corresponds to a region of approximately 200 kb (Fig. 1A).

To identify expressed sequences from the *RPS2* region, we used the cosmid clones 4-6, 4-4, and 7-26 (Fig. 1A) to probe an *Arabidopsis* complementary DNA (cDNA) library (*13*). Eight different classes of cDNAs were isolated. The inferred gene location for five of these cDNAs is shown in Fig. 1B; three additional cDNAs mapped just outside this region. These eight cDNAs were used to screen for altered transcript production in *rps2* mutants in an effort to determine correspondence between one of the cDNAs and *RPS2* (*14*). However, no alterations were detected (*15*).

Further efforts to identify *RPS2* used functional complementation of *Arabidopsis* Col-0 *rps2-201/rps2-201* plants. An additional set of overlapping clones from the *RPS2* region was constructed with a cosmid vector suitable for *Agrobacterium*-mediated transformation (*16*). Three separate transformation methods were used (*17*–*19*), including a modified vacuum infiltration procedure that greatly expedited these efforts (*20*). *RPS2* activity was initially observed in Col-0 *rps2-201/rps2-201* plants transformed with the 18-kb genomic region carried on cosmid pD4 (Fig. 1B). These plants displayed a strong hypersensitive resistance response (HR) when inoculated with *P. syringae* expressing *avrRpt2* but did not develop an HR after inoculation with strains not carrying *avrRpt2*. Disease resistance assays and DNA blots performed on the self-progeny of one pD4 transformant confirmed cosegregation between the resistant phenotype and the introduced DNA (*15*). Col-0 *rps2-201/rps2-201* plants carrying the wild-type genomic region from cosmid pD4 did not display disease symptoms (Fig. 2). Growth of *P. syringae* expressing *avrRpt2* was restricted in the leaf tissue of Col-0

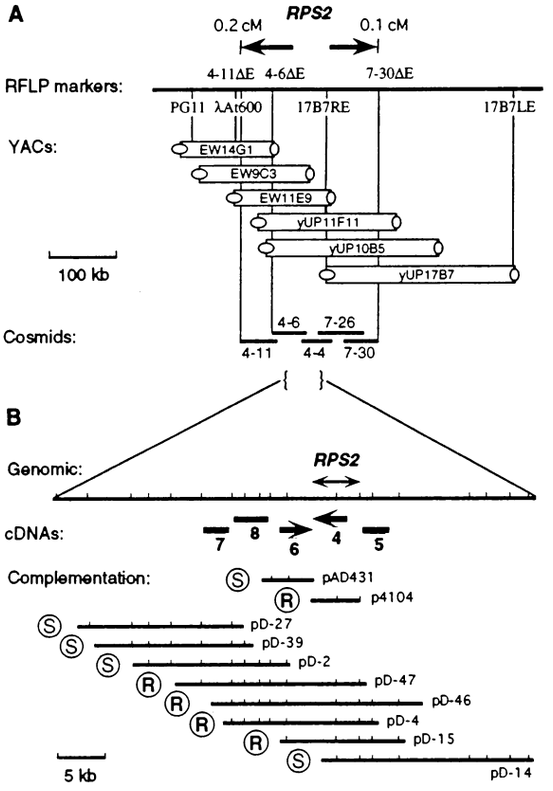

Fig. 1. Genetic and physical map of the *Arabidopsis* genomic region containing *RPS2*, showing location of expressed sequences and *rps2*-complementing plasmids. (**A**) RFLP analysis of a population segregating for *RPS2* and *rps2-201* localized *RPS2* to the region bounded by markers 4-11ΔE and 7-30ΔE. Identification of a set of YAC clones and cosmid clones spanning this region allowed high-resolution RFLP analysis and subsequent subcloning of *RPS2* region DNA (*12*, *38*). (**B**) Five expressed sequences encoded by the region denoted with brackets in (A) were identified (*13*). The location of the genomic region corresponding to each cDNA clone is indicated by thick bars; arrowheads indicate the direction of transcription for cDNA 4 and cDNA 6. Vertical marks denote the Eco RI recognition sites of this genomic region. Genetic transformation of an *Arabidopsis* Col-0 *rps2-201/rps2-201* mutant line with genomic DNAs carried in the pD series binary cosmids (*16*) produced plants with the *avrRpt2*-specific disease resistance phenotype indicated (R, resistant; S, susceptible). Transformation with the cosmid subclones pAD431 and p4104 (*20*, *21*) indicated that cDNA 4 corresponds to *RPS2*.

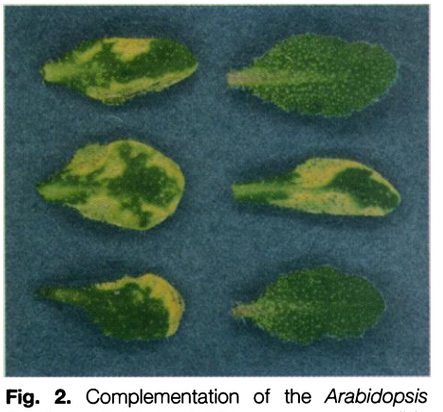

Fig. 2. Complementation of the *Arabidopsis* Col-0 *rps2-201/rps2-201* disease-susceptible phenotype with the cloned *RPS2* locus. *Arabidopsis* leaves were inoculated with *P. syringae* pv. *tomato* strain DC3000 (left column, DC3000 containing plasmid pVSP61 with no insert) or with the same strain expressing *avrRpt2* (right column, *avrRpt2* on plasmid pV288) (*8*). Inoculation was by dipping in bacteria resuspended at an optical density at 600 nm of 0.3 in 10 mM $MgCl_2$ with 0.02% Silwet L-77 (*10*). Top: ecotype Col-0 (*RPS2/RPS2*); middle: Col-0 *rps2-201/rps2-201*; bottom: T_3 individuals from a Col-0 *rps2-201/rps2-201* plant transformed with *RPS2* carried on pD4 (this T_3 family was derived from a T_2 individual plant homozygous for the kanamycin resistance marker adjacent to *RPS2* on pD4).

rps2-201/rps2-201 plants carrying this introduced DNA (T_3-146 of Fig. 3). The resistant phenotype resembled wild-type Col-0. Resistance was dependent on the presence of *avrRpt2* in the pathogen, because all plants used were susceptible to infection by *P. syringae* strains lacking *avrRpt2* (Fig. 2) (*15*). These results indicate that *RPS2* is encoded within the 18-kb *Arabidopsis* genomic region carried on cosmid pD4.

The insert in cosmid pD4 is derived from a region of the genome with a high density of expressed sequences (five in 21 kb) (Fig. 1B). To identify *RPS2*, we used a set of binary cosmids that contain partially overlapping inserts from this region in additional transformation experiments (Fig. 1B) (*20*). The resistance phenotypes of these transformants (Fig. 1B) suggested that *RPS2* activity was contained within cDNA 4 (*21*). Plants homozygous for other susceptible alleles of *RPS2* (*rps2-101N*, *rps2-101C*, *rps2-301*, and ecotype Wü-0) (8, 9), when transformed with p4104, also displayed resistance against *P. syringae* expressing *avrRpt2* (*15*). The gene corresponding to cDNA 4 was therefore designated *RPS2*.

The DNA sequence of *RPS2* was determined for both cDNA 4 and the corresponding genomic region from wild-type Col-0 (*22*). No introns were detected. The *RPS2* sequence predicts a 909–amino acid, 105-kD gene product (Fig. 4). Support for designation of this open reading frame as *RPS2* came both from the complementation experiments discussed above and from sequence analysis of the mutant allele *rps2-201*. The *rps2-201* sequence deviates from that of wild-type *RPS2* by a single-nucleotide change that converts Thr^{668} of this open reading frame to Pro. No other open reading frames are present at the site of the *rps2-201* mutation. Additional evidence supporting designation of this gene as *RPS2* has been obtained by DNA sequence analysis of mutant alleles *rps2-101C*, *rps2-102C*, and *rps2-101N* (*23*). No additional sequences with strong similarity to *RPS2* were observed when blots of genomic DNA from *Arabidopsis*, bean, soybean, tomato, green pepper, tobacco, rice, barley, and maize were probed with a 2.8-kb probe encompassing the *RPS2* open reading frame (*22*).

Analysis of the derived amino acid sequence for *RPS2* revealed several regions with similarity to known polypeptide motifs (*24*). Most prominent among these is a region of leucine-rich repeats (LRRs) (*25*). The LRR motif has been implicated in protein-protein interactions and ligand binding in a diverse array of proteins (*25–29*). LRRs, for example, form the hormone-binding sites of mammalian gonadotropin hormone receptors (*28*) and a domain of yeast adenylate cyclase that interacts with the RAS2 protein (*26*). In *RPS2*, the LRR domain spans amino acids 503 to 809 and contains 13 repeat units of 22 to 26 amino acids in length; a portion of each repeat resembles the consensus (I/L/V)XXLXXLXX(I/L)XL (*30*). Six sequences matching the N-glycosylation consensus [NX(S/T)] (*31*) were observed in *RPS2*, and five of these are within the LRR region (Fig. 4). The single-nucleotide difference between functional *RPS2* and mutant allele *rps2-201* is within the LRR coding region, and this mutation disrupts one of the potential glycosylation sites.

The deduced amino acid sequence for *RPS2* carries a second potential protein-protein interaction domain, a leucine zipper (*32*), at amino acids 30 to 57. This region contains four contiguous heptad repeats that match the consensus sequence (I/R)XDLXXX (*30*). Leucine zippers facilitate the dimerization of transcription factors by formation of a coiled-coil structure, but no sequences suggestive of an adjacent DNA binding domain (such as a strongly basic region or a potential zinc finger) were detected in *RPS2*. Coiled-coil regions also promote specific interactions between proteins that are not transcription factors (*33*), and computer database similarity searches with the region spanning amino acids 30 to 57 of *RPS2* revealed the greatest similarity to the coiled-coil regions of numerous myosin and paramyosin proteins.

The sequence GPGGVGKT (*30*) at deduced amino acids 182 to 189 of *RPS2* precisely matches the generalized consensus for the phosphate-binding loop (P loop) of numerous adenosine triphosphate (ATP)– and guanosine triphosphate (GTP)–binding proteins (*34*). The postulated *RPS2* nucleotide binding site is similar to those found in RAS proteins and ATP synthase β subunits (*34*), but surprisingly is most similar to the published P loop of the *chvD* gene from plant-colonizing *Agrobacterium* (*35*). The presence of this P loop sequence strongly suggests nucleotide triphosphate binding as one aspect of *RPS2* function.

A potential membrane-spanning domain is located at amino acids 340 to 360 of the *RPS2* gene product, which raises the possibility of membrane localization with the NH_2-terminal leucine zipper and P loop domains residing together on the opposite side of the membrane from the LRR region. An orientation in which the COOH-terminal LRR domain is extracellular is suggested

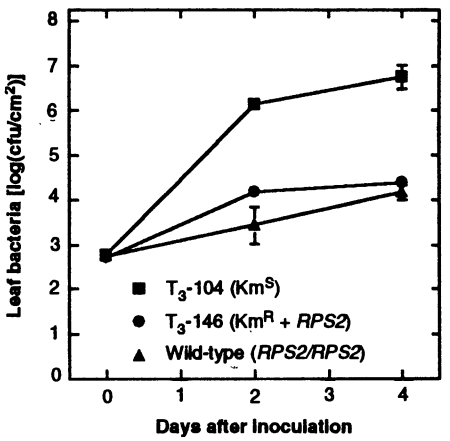

Fig. 3. Growth of *P. syringae* pv. *tomato* strain DC3000 (*avrRpt2*) within an *Arabidopsis rps2* mutant complemented with the cloned *RPS2* gene. "T_3" plant lines were established by selfing the progeny of a single Col-0 *rps2-201/rps2-201* transformant heterozygous for *RPS2* introduced with pD4 (Fig. 1B). T_3-146 plants are from a plant homozygous for the pD4 kanamycin resistance (Km^R) marker (presumably homozygous for the introduced *RPS2*), whereas control plants (T_3-104) are from a kanamycin-susceptible segregant (Km^S). "Wild-type" are *Arabidopsis* Col-0. Plants were inoculated by vacuum infiltration, and bacterial growth in leaves was monitored as described (*10*), except that NYGA (*45*) was used instead of King's B medium. Similar results were obtained in two independent experiments. Sample means and standard errors are depicted for one of these experiments.

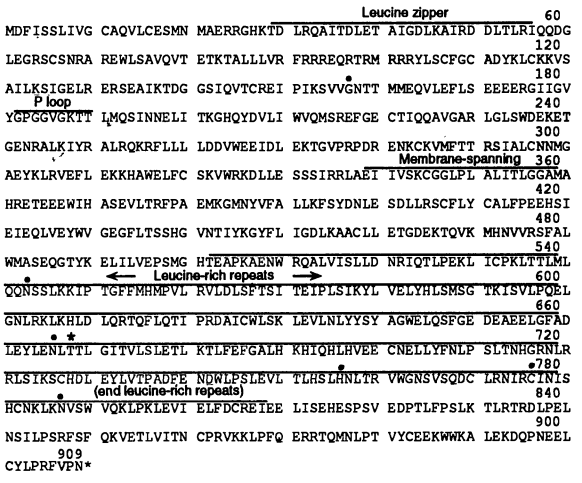

Fig. 4. Derived amino acid sequence of *RPS2* (*30*). Regions with similarity to previously defined functional domains are indicated with a line over the relevant amino acids. Potential N-glycosylation sequences are marked with a dot, and the location of the *rps2-201* Thr to Pro mutation at amino acid 668 is marked with an asterisk.

by the fact that five of six potential N-linked glycosylation sites occur COOH-terminal to the proposed membrane-spanning domain and by the overall more positive charge of the NH_2-terminal amino acid residues (*31*, *36*). A number of proteins that contain LRRs are postulated or known to be membrane-spanning receptors in which the LRRs are displayed extracellularly as a ligand-binding domain (*27–29*).

The plant kingdom contains hundreds of resistance genes that are necessarily divergent because they control different resistance specificities. However, plant defense responses such as production of activated oxygen species, pathogen-response (PR) protein gene expression, and the hypersensitive response are common to diverse plant-pathogen interactions (*4*). This implies that there are points of convergence in the defense signal transduction pathways downstream of initial pathogen recognition and suggests that similar functional motifs will exist among diverse resistance gene products. In support of this hypothesis, *RPS2* has been found to share regions of similarity (including the P loop and leucine-rich repeats) with the recently cloned *N* gene of tobacco (*37*). *RPS2* and *N* represent a new class of disease resistance genes, as they are not similar to the previously described *Hm1* or *Pto* genes (*6*, *7*). It is particularly intriguing to note that whereas *RPS2* confers resistance against bacterial pathogens, *N* encodes resistance against isolates of tobacco mosaic virus (*3*, *37*).

Although the molecular function of *RPS2* in defense signal transduction remains to be elucidated, the *RPS2* sequence predicts a number of testable models. Pathogen avirulence genes have been shown to control the production of resistance gene–specific elicitors of plant defense responses, and resistance genes have long been postulated to encode the receptors for these elicitors (*1*, *2*). Given that LRRs form the extracellular ligand-binding domain of proteins such as the gonadotropin hormone receptors (*28*), the presence of LRRs and a possible transmembrane domain suggest that the *RPS2* gene product may be the receptor of the *avrRpt2*-controlled elicitor. Alternatively, the LRR of *RPS2* may function as an intracellular domain that mediates protein-protein interaction in a downstream step of the signal transduction pathway, as is the case for yeast adenylate cyclase (*26*). The presence of a P loop suggests testing of the *RPS2* gene product for nucleotide triphosphate binding activity. Given that leucine zipper and LRR regions are present in the *RPS2* sequence, it is highly probable that protein-protein interactions are a key component of *RPS2* function. Experiments that examine these models are anticipated to be informative not only regarding *RPS2* function, but more generally regarding the molecular nature of plant defense signal transduction.

REFERENCES AND NOTES

1. N. T. Keen, *Annu. Rev. Genet.* **24**, 447 (1990); J. L. Bennetzen and J. D. G. Jones, in *Genetic Engineering: Principles and Methods*, J. K. Setlow, Ed. (Plenum, New York, 1992), vol. 14, pp. 99–124.
2. N. T. Keen, A. F. Bent, B. J. Staskawicz, in *Application of Biotechnology to Plant Pathogen Control*, I. Chet, Ed. (Wiley, New York, 1993), pp. 65–88.
3. N. T. Keen and W. O. Dawson, in *Genes Involved in Plant Defense*, T. Boller and F. Meins, Eds. (Springer-Verlag, New York, 1992); vol. 8, pp. 76–103.
4. C. J. Lamb, M. A. Lawton, M. Dron, R. A Dixon, *Cell* **56**, 215 (1989); R. A. Dixon and C. J. Lamb, *Annu. Rev. Plant Physiol. Plant Mol. Biol.* **41**, 339 (1990); Z. Klement, in *Phytopathogenic Procaryotes*, M. S. Mount and G. H. Lacy, Eds. (Academic Press, New York, 1982), pp. 149–177.
5. I. Apostol, P. F. Heinstein, P. S. Low, *Plant Physiol.* **90**, 109 (1989); M. M. Atkinson, L. D. Keppler, E. W. Orlandi, C. J. Baker, C. F. Mischke, *ibid.* **92**, 215 (1990); N. Doke, *Physiol. Plant Pathol.* **23**, 345 (1983); G. Felix, D. G. Grosskopf, M. Regenass, T. Boller, *Proc. Natl. Acad. Sci. U.S.A.* **88**, 8831 (1991); R. Vera-Estrella, J. Barkla, V. J. Higgins, E. Blumwald, *Plant Physiol.* **104**, 209 (1994).
6. G. S. Johal and S. P. Briggs, *Science* **258**, 985 (1992).
7. G. B. Martin *et al.*, *ibid.* **262**, 1432 (1993).
8. B. N. Kunkel, A. F. Bent, D. Dahlbeck, R. W. Innes, B. J. Staskawicz, *Plant Cell* **5**, 865 (1993).
9. G.-L. Yu, F. Katagiri, F. M. Ausubel, *Mol. Plant-Microbe Interact.* **6**, 434 (1993).
10. M. Whalen, R. Innes, A. Bent, B. Staskawicz, *Plant Cell* **3**, 49 (1991).
11. R. W. Innes, A. F. Bent, B. N. Kunkel, S. R. Bisgrove, B. J. Staskawicz, *J. Bacteriol.* **175**, 4859 (1993).
12. YAC clones with overlapping insert DNA were isolated from three separate YAC libraries of *Arabidopsis* ecotype Col-0 genomic DNA (*38*, *39*). The contig was extended in both directions from RFLP marker λAt600 and spans approximately 900 kb in the *RPS2* region. Cosmids 4-4, 4-6, 4-11, 7-26, and 7-30 were derived from YACs EW11E4 and EW3H7, which carry *Arabidopsis* ecotype Col-0 genomic DNA (*40*). Genetic mapping used segregating populations from crosses between *RPS2*/*RPS2* (No-0 ecotype) and *rps2-201*/*rps2-201* (Col-0 background) plants. For high-resolution mapping, prescreens for recombinant chromosomes were carried out by genotyping a population of at least 413 individuals [including 294 from (*8*)] with the use of markers 17B7LE or RN23 (*8*) and markers PG11 (*41*) or λAt600 (*42*). For F_2 plants carrying recombinant chromosomes, the *RPS2* genotype was then determined by scoring F_3 families for disease resistance against *P. syringae* strains expressing *avrRpt2* (*8*). DNA blot analysis revealed that the closest recombination breakpoints flanking *RPS2* included two independent crossovers between markers 4-11ΔE and 4-6ΔE and one crossover between markers 7-30ΔE and 17B7RE (Fig. 1A).
13. To allow identification of pathogen-induced as well as constitutive messages, we isolated cDNA clones from a library made with polyadenylated RNA from *Arabidopsis* Col-0 leaf tissue harvested 2.5 to 3.5 hours after inoculation with *P. syringae* pv. *tomato* strain DC3000 expressing *avrRpt2*. *RPS2* region cDNA clones were grouped into eight separate classes with restriction enzyme fingerprinting, and we identified the genomic Eco RI restriction fragments with homology to each cDNA class by probing blots of restricted cosmid DNA (Fig. 1A) with the largest cDNA clone from each class. The genes corresponding to cDNAs 4, 5, 6, 7, and 8 were judged to be single-copy on the basis of blots of restricted *Arabidopsis* genomic DNA probed at moderately high stringency [2× saline sodium citrate (SSC) wash at 65°C] with the largest cDNA clone from each class. The DNA sequence of similar cDNA clones has been determined and deposited with GenBank (*23*).
14. In screens for altered transcript production, blots of total RNA from wild-type Col-0, from *rps2-201*, *rps2-202*, *rps2-203*, and *rps2-301* mutants (*8*), from *rps2-101C* and *rps2-101N* mutants (*9*), and from susceptible ecotypes Wü-0 (*8*) and Po-1 (*10*) were probed with the largest clone from each cDNA class shown in Fig. 1B.
15. A. F. Bent, B. N. Kunkel, D. Dahlbeck, unpublished results.
16. To construct pD series plasmids for plant transformation, we made libraries (average insert size ~20-kb) in binary vector pCLD0451 with size-fractionated yeast DNA from strains carrying the *RPS2* region YAC clones EW11E9, EW9C3, and YUP11F11. Vector pCLD04541 was made by inserting a cos site and the Bluescript polylinker into pSLJ1261 (*43*). pCLD04541 clones carrying *Arabidopsis* DNA were isolated by probing this library with insert DNA from the cosmids 4-4, 4-6, 4-11, 7-26, and 7-30. Forty-five of the resulting pD-series clones were organized into a highly overlapping contig.
17. N. Bechtold, J. Ellis, G. Pelletier, *C.R. Acad. Sci. Paris Life Sci.* **316**, 1194 (1993).
18. S. S. Chang *et al.*, *Plant J.* **5**, 551 (1994).
19. D. Valvekens, M. V. Montague, M. V. Lijsbettens, *Proc. Natl. Acad. Sci. U.S.A.* **85**, 5536 (1988).
20. For plant transformation by vacuum infiltration, the procedure of Bechtold *et al.* (*17*) was modified such that plants were grown in peat-based potting soil covered with a screen, primary inflorescences were removed, and plants with secondary inflorescences (approximately 3 to 15 cm in length) were inverted directly into infiltration medium, infiltrated, and then grown to seed harvest without removal from soil [detailed protocol available on the AAtDB computer database (*44*) or from A.F.B.]. The presence of introduced sequences in the initial pD4 transformant was verified by DNA blot analysis with pD4 vector and insert sequences (separately) as probes. The presence of the expected pCLD04541 sequences in transformants obtained with the vacuum infiltration protocol was also confirmed by DNA blot analysis. Root transformation experiments (*19*) were performed with an easily regenerable *rps2-201*/*rps2-201* plant derived from the Col-0 *rps2-201* × No-0 mapping population. Transformants were obtained for pD4 with in planta transformation (*20*), for pD2, 14, 15, 39, and 49 with root transformation (*19*), and for pD2, 4, 14, 15, 27, and 47 with vacuum infiltration (*17*) as modified above.
21. We constructed pAD431 using pCLD04541 and a genomic 4.0-kb Xba I–Bam HI fragment that contains all of the transcribed cDNA 6 sequence along with 1.1 kb of upstream and 0.1 kb of downstream sequence. We constructed p4104 using pCLD04541 and contiguous genomic 2.4-kb Eco RI and 2.7-kb Eco RI–Cla I fragments that contain all of the transcribed cDNA 4 sequence along with 1.7 kb of upstream and 0.1 kb of downstream sequence. Transformants for pAD431 and p4104 were obtained with the modified vacuum infiltration procedure. For pAD431 (Fig. 1B), 0 out of 19 transformants obtained in three independent experiments displayed disease resistance against *P. syringae* expressing *avrRpt2*. In contrast, 18 transformants obtained in three independent transformation experiments with p4104 (Fig. 1B) developed a clear hypersensitive resistance response after inoculation with *P. syringae* expressing *avrRpt2*.
22. The DNA sequence was determined completely for both strands by the primer walk method, with the use of DyeDeoxy terminator cycle sequencing and the Model 373 DNA sequencing system (Applied Biosystems, La Jolla, CA) as well as ^{35}S-labeled deoxy-ATP and Sequenase (U.S. Biochemical, Cleveland, OH). To determine if additional plant sequences with similarity to *RPS2* could be observed, we probed blots of total genomic plant DNA with a 2.8-kb probe encompassing *RPS2* and washed them 0.5× SSC at 65°C.
23. M. Mindrinos, F. Katagiri, G.-L. Yu, F. Ausubel, *Cell*, in press.
24. Computer searches for similar sequences were

carried out with BlastP [S. F. Altschul *et al.*, *J. Mol. Biol.* **215**, 403 (1990)] v.1.3.11MP and the National Center for Biotechnology Information nonredundant peptide sequence database. The nucleotide sequence encoding *RPS2* has been deposited with GenBank (accession number U14158).
25. B. Kobe and J. Deisenhofer, *Nature* **366**, 751 (1993).
26. N. Suzuki *et al.*, *Proc. Natl. Acad. Sci. U.S.A.* **87**, 8711 (1990).
27. J. A. Lopez *et al.*, *ibid.* **84**, 5615 (1987).
28. T. Braun, P. R. Schofield, R. Sprengel, *EMBO J.* **10**, 1885 (1991).
29. D. S. Schneider, K. L. Hudson, T. Lin, K. V. Anderson, *Genes Dev.* **5**, 797 (1991).
30. Abbreviations for the amino acid residues are: A, Ala; C, Cys; D, Asp; E, Glu; F, Phe; G, Gly; H, His; I, Ile; K, Lys; L, Leu; M, Met; N, Asn; P, Pro; Q, Gln; R, Arg; S, Ser; T, Thr; V, Val; W, Trp; and Y, Tyr. X indicates any amino acid.
31. R. Kornfeld and S. Kornfeld, *Annu. Rev. Biochem.* **54**, 631 (1985).
32. T. Alber, *Curr. Opin. Gen. Dev.* **2**, 205 (1992).
33. A. Lupas, M. Van Dyke, J. Stock, *Science* **252**, 1162 (1991).
34. M. Saraste, P. R. Sibbald, A. Wittinghofer, *Trends Biochem. Sci.* **15**, 430 (1990).
35. S. C. Winans, R. A. Kerstetter, E. W. Nester, *J. Bacteriol.* **170**, 4047 (1988).
36. G. von Heijne, *J. Mol. Biol* **225**, 487 (1992).
37. S. Whitham *et al.*, *Cell*, in press.
38. S. Gibson and C. Somerville, in *Methods in* Arabidopsis *Research*, C. Koncz, N.-H. Chua, J. Schell, Eds. (World Scientific, London, 1992), pp. 119–143.
39. E. R. Ward and G. C. Jen, *Plant Mol. Biol.* **14**, 561 (1990); J. R. Ecker, *Methods* **1**, 186 (1990); E. Grill and C. Somerville, *Mol. Gen. Genet.* **226**, 484 (1991).
40. J. Leung *et al.*, *Science* **264**, 1448 (1994).
41. A. Konieczny and F. M. Ausubel, *Plant J.* **4**, 403 (1993).
42. C. Chang, J. L. Bowman, A. W. DeJohn, E. S. Lander, E. M. Meyerowitz, *Proc. Natl. Acad. Sci. U.S.A.* **85**, 6856 (1988).
43. J. D. G. Jones *et al.*, *Transgenic Res.* **1**, 285 (1992).
44. J. M. Cherry, S. W. Cartinhour, H. M. Goodman, *Plant Mol. Biol. Report.* **10**, 308 (1992).
45. M. J. Daniels, C. E. Barber, D. C. Turner, S. G. Cleary, M. K. Sawzyc, *J. Gen. Microbiol.* **130**, 2447 (1984).
46. A.F.B. and B.N.K. contributed equally to this work. We thank T. Tai for the cDNA library, G.-L. Yu and M. Mindrinos for the *rps2-101C* and *rps2-101N* mutants, and C. Lister and C. Dean for vector pCLD04541. We also thank M. Mindrinos, F. Katagiri, G.-L. Yu, F. Ausubel, and B. Baker for sharing results before publication and C. Dean for her support during construction of the YAC contig. Supported in part by grants from the U.S. Department of Energy (B.J.S.), C.N.R.S. (J.G.), and the American Cancer Society, California Division Postdoctoral Fellowship (B.N.K.).

25 July 1994; accepted 1 September 1994

Thymus-Neuroendocrine Interactions in Extrathymic T Cell Development

Jin Wang and John R. Klein*

Studies of the development of murine intestinal intraepithelial lymphocytes (IELs) have yielded markedly different results depending on the experimental system used. In athymic radiation chimeras, IELs consist of all subsets found in euthymic mice; adult mice that were athymic at birth have only IELs that are positive for T cell receptor γδ and CD8αα. These differences are resolved by the finding that administration of the neuropeptide thyrotropin-releasing hormone to adult mice thymectomized as neonates leads to the development of all IEL T cells. Thus, a neuroendocrine signal initiated by the thymus during fetal or neonatal life appears to be required for subsequent extrathymic maturation of gut αβ T cells.

There now is considerable evidence that some, or possibly all, murine intestinal IELs are T cells that have matured independent of the thymus (*1–4*), thereby constituting the largest group of peripheral extrathymic T cells. Yet, opinions differ sharply as to which IELs are thymus-dependent and which are thymus-independent (*5*, *6*); those differences primarily reflect the particular experimental system used—that is, whether mice were made athymic as adults (athymic radiation chimeras) (*2*, *3*) or whether they were athymic from birth (*4*, *6*). Understanding the basis for those differences is essential for determining which IELs are truly extrathymic T cells and for understanding which experimental system most accurately reflects the biology of the IELs in normal mice. In that context, several studies have recently reported that engraftment into neonatally athymic mice with fetal thymus or with thymus tissues contained in diffusion chambers (*6*) leads to the appearance of αβ T cells in the gut. Because in the latter experiments lymphocytes could not enter the engrafted thymus tissue, it was concluded that the thymus stroma directly influences the development of αβ T cells within the gut. As reported here, however, a similar outcome can be achieved by neurohormone supplementation in the absence of thymus engraftment, which suggests that although the thymus is involved in some stage of that process, it is not directly responsible for the development of gut αβ T cells.

We isolated IELs from adult athymic radiation chimeras and from adult neonatally thymectomized (NTX) mice (*7*) and compared them for expression of lymphocyte markers by flow cytometric analyses (*8*) to IELs from normal euthymic mice (that is, mice with normal thymuses). Because most TCRαβ, CD8αβ, and CD5 IELs express Thy-1 (*9*, *10*) and because those populations were of particular interest in our study, the hematopoietic origins of IELs in athymic chimeras were determined with irradiated CBA (Thy-1.2) congenic mice injected with bone marrow from AKR (Thy-1.1) mice. More than 90% of Thy-1$^+$ IELs in athymic chimeras expressed the Thy-1.1 allele, which indicates that they were donor-derived lymphocytes and that they were not residual host cells (Fig. 1). IELs from athymic chimeras (Fig. 2B) expressed all subsets that existed in euthymic mice (Fig. 2A). In those mice, IELs consisted of both TCRαβ$^+$CD5$^+$ cells and TCRγδ$^+$CD5$^-$ cells. Virtually all CD8β$^+$ IELs were Thy-1$^+$ cells, and both CD8αα and CD8αβ IELs were present. CD5 was expressed on some, though not all, TCRαβ$^+$ IELs; TCRγδ$^+$ IELs were primarily CD5$^-$. Consistent with findings from this (*2*) and other laboratories (*3*), T cells were absent in peripheral immune compartments outside the intestine. These findings indicate that despite a reduction in the proportion of some types of IELs in athymic chimeras (for example, CD8αβ$^+$ and Thy-1$^+$CD8β$^+$ cells) (Fig. 2B), all IEL subsets nonetheless developed in the absence of the thymus.

In contrast to IELs in euthymic mice and athymic chimeras, IELs in NTX mice consisted of only TCRγδ$^+$CD8αα$^+$ cells (Fig. 2C). Additionally, more than half of the IELs in NTX mice were devoid of markers of mature lymphocytes and, even among the TCRγδ$^+$ IELs, there was a reduction in the proportion of TCRγδ IELs in NTX mice compared to the number of IELs from athymic chimeras (Fig. 2). However, the most striking difference between IELs in athymic chimeras and those in NTX mice was the absence of TCRαβ, CD8αβ, Thy-1, and CD5 cells, a finding that was consistent in several IEL isolates from NTX mice. Thus, IELs in mice that are athymic at birth lack αβ T cells.

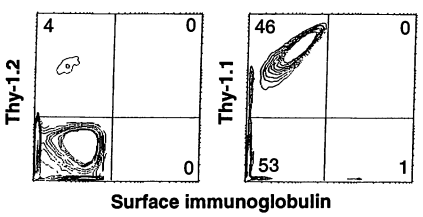

Fig. 1. Expression of Thy-1.1 and Thy-1.2 on IELs from CBA athymic radiation chimeras injected with AKR bone marrow (*7*).

Department of Biological Science and Mervin Bovaird Center for Studies in Molecular Biology and Biotechnology, University of Tulsa, Tulsa, OK 74104, USA.

*To whom correspondence should be addressed.